PROCEEDINGS OF SCIENCE

ONLINE ICRC 2021
THE ASTROPARTICLE PHYSICS CONFERENCE
Berlin | Germany
37th International Cosmic Ray Conference
12–23 July 2021

# Dissecting the inner Galaxy with gamma-ray pixel count statistics

**Silvia Manconi,**[a,*] **Francesca Calore**[b] **and Fiorenza Donato**[c,d]

[a] *Institut für Theoretische Teilchenphysik und Kosmologie, RWTH Aachen University, Germany*
[b] *Univ. Grenoble Alpes, USMB, CNRS, LAPTh, F-74940 Annecy, France*
[c] *Dipartimento di Fisica, Università di Torino, via P. Giuria, 1, I-10125 Torino, Italy*
[d] *Istituto Nazionale di Fisica Nucleare, Sezione di Torino, via P. Giuria, 1, I-10125 Torino, Italy*
*E-mail:* manconi@physik.rwth-aachen.de

The nature of the GeV gamma-ray Galactic center excess (GCE) in the data of Fermi-LAT is still under investigation. Different techniques, such as template fitting and photon-count statistical methods, have been applied in the past few years in order to disentangle between a GCE coming from sub-threshold point sources or rather from diffuse emissions, such as the dark matter annihilation in the Galactic halo. A major limit to all these studies is the modeling of the Galactic diffuse foreground, and the impact of residual mis-modeled emission on the results' robustness. We combine for the first time adaptive template fitting and pixel-count statistical methods in order to assess the role of sub-threshold point sources to the GCE, while minimizing the mis-modelling of diffuse emission components. We reconstruct the flux distribution of point sources in the inner Galaxy well below the Fermi-LAT detection threshold, and measure their radial and longitudinal profiles. We find that point sources and diffuse emission from the Galactic bulge each contributes about 10% of the total emission therein, disclosing a sub-threshold point-source contribution to the GCE.

*37th International Cosmic Ray Conference (ICRC 2021)*
*July 12th – 23rd, 2021*
*Online – Berlin, Germany*

*Presenter





PoS(ICRC2021)677

## 1. Introduction

The Galactic center excess (GCE) is an unexpected $\gamma$-ray component detected at GeV energies from the inner degrees of the Galaxy in the data of the Large Area Telescope (LAT) aboard the *Fermi* satellite, see the recent review in [1] and references therein. The GCE discovery raised a great interest in the community, and its nature is still under investigation. While the GCE morphology has been found to be consistent with a Navarro, Frenk and White (NFW) profile for annihilating particle dark matter (DM), see e.g. [1–3], it could also be due to a population of millisecond pulsars [4]. Stellar distributions were used as tracers of point sources (PS) emitting below threshold, and turned out to match the morphological features of GCE photons better than DM-inspired templates [5–7]. Complementary studies of photon-count statistics revealed initially that the GCE can be entirely due to a population of PS [8]. Recently, the DM interpretation was brought back [9], although hampered by systematics affecting photon-count statistical methods [10–14]. A major limitation to all these studies is the modeling of the Galactic diffuse foreground, and the impact of residual mis-modeled emission on the results' robustness. As for template fitting methods, the analysis of the diffuse emission has been recently approached with the `skyFACT` algorithm, which fits the $\gamma$-ray sky by combining methods of image reconstruction and adaptive spatio-spectral template regression [15]. The `skyFACT` method has been tested in the *Inner Galaxy* (IG) region, and probed to be efficient in the removal of most residual emission for a robust assessment of the GCE properties [5, 15]. Another source of uncertainty is the contribution of sub-threshold PSs. Photon-count statistical methods can discriminate photons from $\gamma$-ray sources based on their statistical properties. In particular, the 1-point probability distribution function method [16] (`1pPDF`) fits the contribution of diffuse and PS components to the $\gamma$-ray 1-point fluctuations histogram. Employing `1pPDF` on *Fermi*-LAT data, it was possible to measure the PS count distribution per unit flux, $dN/dS$, below the LAT detection threshold at high latitudes [16–18], and to set competitive bounds on DM [19].

We here apply the `1pPDF` method to *Fermi*-LAT data from the IG to understand the role of faint PS to the GCE, while minimizing the mis-modelling of diffuse emission components. To this end, we adopt a hybrid approach which combines, for the first time [20], adaptive template fitting methods as implemented in `skyFACT`, and `1pPDF` techniques.

## 2. Data and methods

We analyze 639 weeks of `P8R3 ULTRACLEANVETO` *Fermi*-LAT data [1] until 2020-08-27. For the `skyFACT` fit, we consider an ROI of $40^\circ \times 40^\circ$ around the GC [2], and the 0.3 – 300 GeV energy range. We closely follow [5] and update the analysis for the increased data set and 4FGL catalog [21]. The emission model includes $\gamma$ rays from inverse Compton scattering, $\pi^0$ decay, 4FGL point-like and extended sources, the *Fermi* bubbles, the isotropic $\gamma$-ray background (IGRB), and the GCE. For the latter, we consider a template for the Galactic bulge emission as in [5], and one for a generalized NFW DM distribution with slope 1.26 (NFW126) [22]. We refer to [20] for more details. We follow a two-step procedure: First, we fit $\gamma$-ray data with `skyFACT` in order to build a model for the emission in the region of interest (ROI), maximally reducing residuals found to bias

[1] Publicly available at https://heasarc.gsfc.nasa.gov/\FTP/fermi/data/lat/weekly/photon/.

[2] This ROI still allows to discriminate the GCE morphology without suffering from systematics induced by selecting too narrow ROIs [7].

photon-count statistical methods [12]. Secondly, we run `1pPDF` fits with `skyFACT`-optimized diffuse models as input, and assess the role of PS to the GCE. We operate the `1pPDF` analysis in the energy range 2 – 5 GeV [17, 19], restricting to events with best angular reconstruction (evtype=PSF3) and coming from the inner $20^\circ \times 20^\circ$, IG ROI hereafter. We cut at latitudes $|b| > 0.5^\circ$ or $2^\circ$ to check the stability of `1pPDF` results. The `1pPDF`-fit model components are: An IGRB template (free normalization), a diffuse emission template (free normalization), and an isotropic PS (IPS) population with $dN/dS$ defined by a multiple broken power law with free parameters being the overall normalization $A_S$, the flux break positions, and the broken power-law indices, $n_i$ [20]. The IPS $dN/dS$ measured by the `1pPDF` fit should recover the $dN/dS$ of *Fermi*-LAT detected PS in the bright regime while pushing the PS detection threshold down to lower fluxes [16, 17]. Our goal being to quantify the role of PS to the GCE within the `1pPDF`, we add a *GCE smooth template* with free normalization in the `1pPDF` fit. As a baseline, we use the best-fit `skyFACT` bulge template in the `1pPDF` fit (`1pPDF-B`), and we define the `sF-B` diffuse model as the sum of best-fit inverse Compton, $\pi^0$ decay, *Fermi* bubbles, and extended sources, thus subtracting the bulge emission. The normalization, $A_{B/NFW126}$ for the bulge/NFW126 template, refers to the rescaling factor relative to the best-fit normalization from `skyFACT`. On the one hand, the use of `skyFACT` best-fit diffuse model guarantees a robust characterization of GCE spectrum and morphology against systematics related to the mis-modeling of the diffuse emission [12, 22], resolving over/under-subtraction issues by including a large number of nuisance parameters. The limitations of such a systematic uncertainty are indeed also relevant for the reconstruction of faint PS with `1pPDF` methods. On the other hand, the `skyFACT` optimization procedure mitigates possible systematics related to the mis-modeling of unaccounted components [10], by allowing spatial re-modulation in the fit templates. Besides the bulge, we also consider NFW126 as smooth GCE in the `1pPDF` analysis (`1pPDF-NFW126`). In this case, we construct the corresponding `skyFACT`-optimized diffuse model (`sF-NFW126`) from the `skyFACT` run adopting NFW126 as GCE, in analogy with the `sF-B` model. Such a procedure guarantees maximal consistency between GCE and diffuse models adopted as input in the `1pPDF`. Finally, to bracket the uncertainties related to the optimization of the diffuse model, we also build a `skyFACT`-optimized diffuse template from the `skyFACT` run not including any GCE additional template (`sF-noGCE`).

## 3. Results

*Inner Galaxy: `skyFACT` and `1pPDF` fits.* We first update the `skyFACT` analysis of the IG to the new *Fermi*-LAT dataset, confirming previous results [5–7]. A bulge distribution for GCE photons is strongly preferred by data on top of the NFW126-only model ($\sim 10\sigma$), and there is mild evidence for an additional NFW126 contribution on top of the bulge-only model ($\sim 4\sigma$).

We then use `skyFACT`-optimized diffuse and smooth GCE templates as input for `1pPDF` fits. Our results for a latitude cut of $2^\circ$ are summarized in Fig. 1, where we show the best-fit $dN/dS$ for the IPS in the IG ROI for several `1pPDF` fit configurations. First, we notice that whatever GCE template is added to the `1pPDF` fit components (bulge or NFW126), its normalization never converges toward the lower bound of its prior interval, regardless of the `skyFACT` diffuse template adopted. The same is valid for the IPS normalization. In all fit setups shown, an IPS population is recovered below the LAT flux threshold. The reconstructed IPS $dN/dS$ is stable against systematics related to the choice

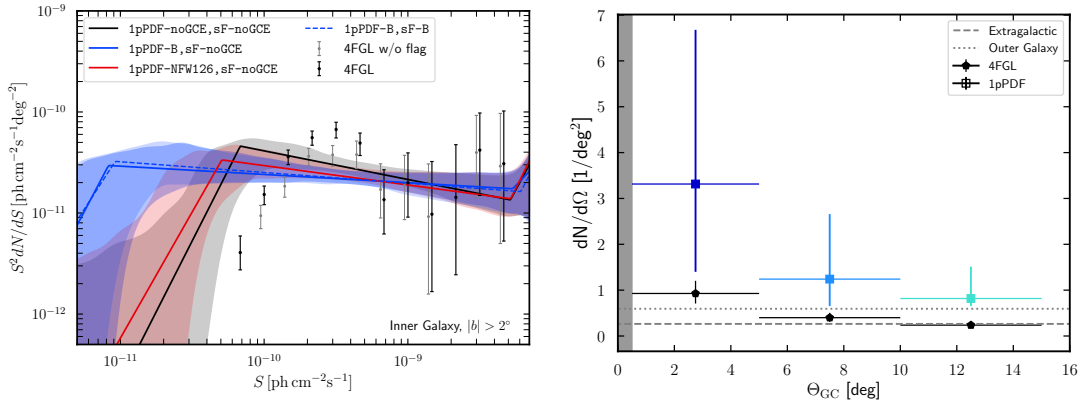


**Figure 1:** *Left: IPS source count distribution in the IG ROI* from the 1pPDF fit for $|b| > 2°$. Solid (dashed) lines correspond to sF-noGCE (sF-B) diffuse template. The black line illustrates the 1pPDF-noGCE case. The blue (red) line refers to 1pPDF-B (1pPDF-NFW126) case. The colored areas correspond to $1\sigma$ uncertainty bands. The black (gray) points represent the count distribution of 4FGL sources (without any analysis flag, see [21]). Right: *Radial source density $dN/d\Omega$ profiles*, as reconstructed by the 1pPDF-B fit using the sF-B diffuse model. We also display source density profiles for 4FGL sources (black points), and average source densities in the OG and EG ROIs.

of skyFACT-optimized diffuse template, and latitude cut. Moreover, it does not present any spurious effect at the *Fermi*-LAT threshold ($\sim 10^{-10}$ ph cm$^{-2}$ s$^{-1}$), and IPS are resolved down to $\sim 10^{-11}$ ph cm$^{-2}$ s$^{-1}$ for $|b| > 0.5°$, depending on the modeling of the smooth GCE component. This holds true even when no GCE smooth template is included neither in the skyFACT fit nor in the 1pPDF one, contrary to what happens using non-optimized diffuse models [10, 12]. We therefore demonstrate, also in the context of 1pPDF methods, that reducing large-scale residuals from mis-modeling of the diffuse emission improves the reconstruction of PS $dN/dS$. When an NFW126 template is included in the 1pPDF fit, the IPS $dN/dS$ is compatible with the 1pPDF-noGCE case. In both cases, the second break in the $dN/dS$ – in addition to the one set in the bright regime – is recovered close to the LAT flux threshold. Instead, the 1pPDF-B reconstructs PS down to lower fluxes, regardless of sF-noGCE or sF-B diffuse models. We quantify now the evidence for models with an additional smooth GCE template. To this end, we compare the global evidence, $\ln \mathcal{Z}$, for the 1pPDF-noGCE, 1pPDF-B and 1pPDF-NFW126 setups, with different skyFACT diffuse model inputs. For each model combination, we compute the Bayes factor between model $i$ and $j$, $B_{ij} = \exp(\ln \mathcal{Z}_i - \ln \mathcal{Z}_j)$, and assess the strength of evidence of model $i$ with respect to model $j$. Detailed results for the different latitude cuts are reported in Tab.1 in [20]. Regardless of the skyFACT-optimized diffuse template adopted, data *always* more strongly support models which include an additional smooth template for the bulge with respect to models without GCE in the skyFACT and/or 1pPDF fits ($\ln B_{ij} > 20$), *and* models with an additional smooth NFW126 component in the skyFACT and/or 1pPDF fits. Whenever a bulge template is included in our analysis, this is preferred even with respect to additional smooth DM templates. As for $|b| > 2°$, the evidence for an additional bulge template (1pPDF-B), with respect to 1pPDF-noGCE is $\ln B \sim 95$. Moreover, in this case the normalization of the bulge template is $A_B = 1.1 \pm 0.1$, supporting the consistency between GCE and diffuse model

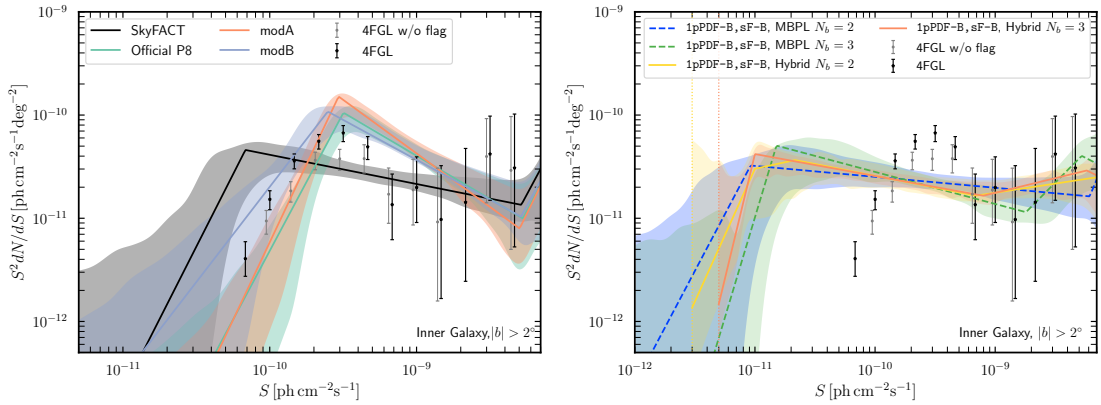


**Figure 2:** *Systematic for dN/dS reconstruction in the IG.* Source count distribution of the IG obtained from the 1pPDF analysis cutting the inner 2°. Left panel: Diffuse emission systematics. The black line is obtained from the `1pPDF` when using the model for the Galactic diffuse emission obtained from `skyFACT` (without any component modeling the GCE, `sF-noGCE`). The colored lines are instead obtained from the `1pPDF` using the official *Fermi*-LAT model for `Pass 8` (cyan line), or modA and modB (orange and indaco lines). Right panel: Effect of the number of free breaks $N_b$ (dashed lines) and of the Hybrid fit approach with different number of breaks and varying the node position. The dotted line illustrates the position of $S_{nd1}$ for the corresponding Hybrid fit.

adopted. We note that, when we use the `sF-noGCE` diffuse model in the `1pPDF` fit including the bulge (`1pPDF-B`), we find comparable evidence to the `1pPDF-B`, `sF-B` setup. Indeed, `skyFACT` is able to re-absorb part of the photons from the bulge by re-modulating (spatially) other diffuse templates, and so, partially reduces the residuals also in the `sF-noGCE` case. Models with PS *and* a smooth bulge component are therefore strongly preferred by data, regardless of the optimized diffuse model employed. On the contrary, the evidence for an additional smooth NFW126 template with respect to models without GCE in the `skyFACT` fit and/or `1pPDF` fits depends on the choice of the `skyFACT`-optimized diffuse template adopted, as well as on the latitude cut.

*Characterizing the faint IPS component.* We also measure the IPS dN/dS in two control regions: The outer Galaxy (OG, $|b| < 20°$, $60° < |l| < 90°$) and the extragalactic region (EG, $|b| > 40°$, $|l| > 90°$). We compute the source density $dN/d\Omega$ in the flux interval $[10^{-11} - 10^{-9}]$ ph cm$^{-2}$ s$^{-1}$, finding $\sim 0.6$ sources/deg$^2$ in the OG, and $\sim 0.3$ sources/deg$^2$ in the EG. Since the spatial distribution of PS is *isotropic* by construction, we test the PS spatial behavior by dissecting the IG ROI into three concentric annuli, masked for latitudes $|b| < 0.5°$. We extract the $dN/dS$ separately in each ring, and integrate it over the flux interval $[10^{-11} - 10^{-9}]$ ph cm$^{-2}$ s$^{-1}$. The result is reported in Fig. 1 as a function of the mean $\Theta_{GC} = \sqrt{b^2 + l^2}$ in each ring, for our baseline `1pPDF-B`, `sF-B` setup. We observe a decreasing trend of the $dN/d\Omega$ in the IG with $\Theta_{GC}$. Also, the $dN/d\Omega$ in the innermost ring is about a factor of three higher than 4FGL sources, as well as than in OG and EG. For the most external ring, the source density is instead comparable with the catalog, OG and EG ones. This corroborates the evidence that the IG PS population is *not purely isotropic nor extragalactic* in origin, but rather it peaks towards the GC. We also build the longitude profile of IG PS, see [20]. The `1pPDF` fits to *Fermi*-LAT data find non-null (and even comparable) emission from both the IPS population *and* the smooth GCE template, in most cases each contributing about

10% of the total emission in the ROI. Since 4FGL sources (2° cut, without analysis flag, see Fig. 1) account for 7% (10% including flagged sources) of the total IG emission, the remaining flux comes from sub-threshold IPS. We have verified [20] that our results are not driven by PS in the ultra-faint regime [11], where the sensitivity of the `1pPDF` method drops (as quantified by the magnitude of uncertainty bands in Fig. 1), and an IPS population may become degenerate with a truly diffuse emission.

*Systematics.* The stability of the $dN/dS$ results in the IG from the combined `1pPDF-skyFACT` analysis of *Fermi*-LAT data was tested against a number of systematics, including the ones from the diffuse emission templates and the $dN/dS$ modeling, extensively discussed in [20]. We apply the `1pPDF` to the IG using other widely used diffuse emission templates: The official spatial and spectral template released by the *Fermi*-LAT Collaboration for `Pass 8` data (Official P8) (`gll_iem_v06.fits`, see Ref. [23]), and the models labeled A (modA) and B (modB), optimized for the study of the IGRB in [24]. By using standard diffuse models (modA, modB and Official P8), we reconstruct spurious sources at $\sim 4 \times 10^{-10}$ ph cm$^{-2}$ s$^{-1}$, well above the sensitivity of the `1pPDF`, see Fig.2 (left panel). Such a peak of the IPS $dN/dS$ disappears instead if we use diffuse emission templates as optimized with `skyFACT`. Large scale residuals are indeed reduced when allowing the spatial diffuse templates to be remodulated in the fit. Even in the absence of an additional GCE template, the `skyFACT` fit remodulates the diffuse components such to partially absorbs GCE photons, therefore reducing residuals and improving the fit with respect to standard diffuse models. Also, in this ROI, all the diffuse models, except the `skyFACT` one, do not properly reproduce the 4FGL catalog bright sources. We therefore confirm previous findings [12] that large residuals due to mis-modelling of diffuse emission induce a bias in the reconstruction of PS in the inner Galaxy. We also identify spatially critical regions within the IG where this mis-modeling effect is more pronounced, notably the Northern hemisphere (both West and East quadrants) [20]. We also verified that the an additional free break is not preferred by data, and that the MBPL obtained with three free breaks is compatible, within the uncertainties, with the case of two free breaks, see Fig. 2 (right panel). To test for possible effects connected to the faint end of the source-count distribution, we repeated the main analysis using the hybrid approach introduced in [16]. We set a fixed node at $S_{\rm nd1}$, with the index of the power-law component below the last node, $n_f = -10$, thus effectively suppressing possible contributions in the ultra-faint regime below the fixed node. Results are summarized in the right panel of Fig. 2 for different values for the position of $S_{\rm nd1}$ in the faint source regime. To the extent we have tested, a node in the faint source regime at $3 - 5 \cdot 10^{-12}$ ph cm$^{-2}$ s$^{-1}$ does not affect the reconstructed $dN/dS$ of the IG, which is well compatible, within $1\sigma$ uncertainty bands, with the benchmark results discussed in Fig. 1. In particular, the $dN/dS$ is well compatible in the flux interval $10^{-11} - 10^{-9}$ ph cm$^{-2}$ s$^{-1}$ , where the radial and longitude profiles are computed.

## 4. Conclusions

The updated `skyFACT` analysis of the IG confirms that the GCE is better described by a bulge template than an NFW126 model at high significance. Moreover, we find that the `1pPDF` method, supplied with `skyFACT` diffuse emission templates, always recovers an IPS population well below the *Fermi*-LAT flux threshold, down to $\sim 10^{-11}$ ph cm$^{-2}$ s$^{-1}$ for $|b| > 0.5°$. The reconstructed IPS $dN/dS$ is stable against a number of systematics, in particular related to the choice of `skyFACT`-

optimized diffuse template and latitude cut. Regardless of the `skyFACT`-optimized diffuse template, data *always* prefer models which include an additional smooth template for the bulge with respect to both models without it and models with an additional NFW126 template, in the `skyFACT` and/or `1pPDF` fits. Our results show that, within the statistical validity of the `1pPDF` and the setups tested, IPS and diffuse bulge each contributes about $O(10\%)$ to the $\gamma$-ray emission along the lines-of-sight toward the GC. In particular, within our baseline model the `1pPDF` founds that PS (bulge) contribute 13% (10%) of the total emission of the IG. Subtracting the contribution from cataloged sources, a non-negligible fraction of the IG emission is accounted by sub-threshold PS. We also verified that this IPS population is not purely isotropic nor extragalactic in origin, rather it peaks towards the very GC. This further corroborates a possible, at least partial, stellar origin of the GCE.

## References

[1] S. Murgia, *The Fermi–LAT Galactic Center Excess: Evidence of Annihilating Dark Matter?*, *Ann. Rev. Nucl. Part. Sci.* **70** (2020) 455–483.

[2] F. Calore, I. Cholis, C. McCabe, and C. Weniger, *A Tale of Tails: Dark Matter Interpretations of the Fermi GeV Excess in Light of Background Model Systematics*, *Phys. Rev.* **D91** (2015), no. 6 063003, [1411.4647].

[3] M. Di Mauro, *The characteristics of the Galactic center excess measured with 11 years of Fermi-LAT data*, 2101.04694.

[4] K. N. Abazajian, *The Consistency of Fermi-LAT Observations of the Galactic Center with a Millisecond Pulsar Population in the Central Stellar Cluster*, *Journal of Cosmology and Astroparticle Physics* **1103** (2011) 010, [1011.4275].

[5] R. Bartels, E. Storm, C. Weniger, and F. Calore, *The Fermi-LAT GeV excess as a tracer of stellar mass in the Galactic bulge*, *Nature Astronomy* **2** (Aug., 2018) 819–828, [1711.04778].

[6] O. Macias, C. Gordon, R. M. Crocker, B. Coleman, D. Paterson, et al., *Galactic bulge preferred over dark matter for the Galactic centre gamma-ray excess*, *Nature Astronomy* **2** (2018), no. 5 387–392, [1611.06644].

[7] O. Macias, S. Horiuchi, M. Kaplinghat, C. Gordon, R. M. Crocker, et al., *Strong Evidence that the Galactic Bulge is Shining in Gamma Rays*, *JCAP* **09** (2019) 042, [1901.03822].

[8] S. K. Lee, M. Lisanti, B. R. Safdi, T. R. Slatyer, and W. Xue, *Evidence for Unresolved Gamma-Ray Point Sources in the Inner Galaxy*, *Phys. Rev. Lett.* **116** (2016) 051103, [1506.05124].

[9] R. K. Leane and T. R. Slatyer, *Revival of the Dark Matter Hypothesis for the Galactic Center Gamma-Ray Excess*, *Phys. Rev. Lett.* **123** (2019), no. 24 241101, [1904.08430].

[10] R. K. Leane and T. R. Slatyer, *Spurious Point Source Signals in the Galactic Center Excess*, *Phys. Rev. Lett.* **125** (2020), no. 12 121105, [2002.12370].

[11] L. J. Chang, S. Mishra-Sharma, M. Lisanti, M. Buschmann, N. L. Rodd, et al., *Characterizing the nature of the unresolved point sources in the Galactic Center: An assessment of systematic uncertainties*, *Phys. Rev. D* **101** (2020), no. 2 023014, [1908.10874].

[12] M. Buschmann, N. L. Rodd, B. R. Safdi, L. J. Chang, S. Mishra-Sharma, et al., *Foreground Mismodeling and the Point Source Explanation of the Fermi Galactic Center Excess*, *Phys. Rev. D* **102** (2020), no. 2 023023, [2002.12373].

[13] Y.-M. Zhong, S. D. McDermott, I. Cholis, and P. J. Fox, *Testing the Sensitivity of the Galactic Center Excess to the Point Source Mask*, *Phys. Rev. Lett.* **124** (2020), no. 23 231103, [1911.12369].

[14] R. K. Leane and T. R. Slatyer, *The enigmatic Galactic Center excess: Spurious point sources and signal mismodeling*, *Phys. Rev. D* **102** (2020), no. 6 063019, [2002.12371].

[15] E. Storm, C. Weniger, and F. Calore, *SkyFACT: High-dimensional modeling of gamma-ray emission with adaptive templates and penalized likelihoods*, *JCAP* **08** (2017) 022, [1705.04065].

[16] H.-S. Zechlin, A. Cuoco, F. Donato, N. Fornengo, and A. Vittino, *Unveiling the Gamma-ray Source Count Distribution Below the Fermi Detection Limit with Photon Statistics*, *Astrophys. J. Suppl.* **225** (2016), no. 2 18, [1512.07190].

[17] H.-S. Zechlin, A. Cuoco, F. Donato, N. Fornengo, and M. Regis, *Statistical Measurement of the Gamma-ray Source-count Distribution as a Function of Energy*, *Astrophys. J. Lett.* **826** (2016), no. 2 L31, [1605.04256].

[18] S. Manconi, M. Korsmeier, F. Donato, N. Fornengo, M. Regis, et al., *Testing gamma-ray models of blazars in the extragalactic sky*, *Phys. Rev. D* **101** (2020), no. 10 103026, [1912.01622].

[19] H.-S. Zechlin, S. Manconi, and F. Donato, *Constraining Galactic dark matter with gamma-ray pixel counts statistics*, *Phys. Rev. D* **98** (2018), no. 8 083022, [1710.01506].

[20] F. Calore, F. Donato, and S. Manconi, *Dissecting the inner Galaxy with $\gamma$-ray pixel count statistics*, 2102.12497.

[21] **Fermi-LAT Collaboration**, S. Abdollahi et al., *Fermi Large Area Telescope Fourth Source Catalog*, *Astrophys. J. Suppl.* **247** (2020), no. 1 33, [1902.10045].

[22] F. Calore, I. Cholis, and C. Weniger, *Background Model Systematics for the Fermi GeV Excess*, *JCAP* **03** (2015) 038, [1409.0042].

[23] F. Acero et al., *Development of the Model of Galactic Interstellar Emission for Standard Point-source Analysis of Fermi Large Area Telescope Data*, *ApJS* **223** (Apr., 2016) 26, [1602.07246].

[24] M. Ackermann et al., *The Spectrum of Isotropic Diffuse Gamma-Ray Emission between 100 MeV and 820 GeV*, *ApJ* **799** (Jan., 2015) 86, [1410.3696].